MULTIDISCIPLINARY DESIGN OPTIMIZATION OF AUTOMOTIVE CRASHWORTHINESS AND NVH USING LS-OPT

K.J. Craig[1,*], Nielen Stander[2], D.A. Dooge[3] and S. Varadappa[4]
[1] Multidisciplinary Design Optimization Group (MDOG), Department of Mechanical and Aeronautical Engineering, University of Pretoria, Pretoria 0002, South Africa
ken.craig@eng.up.ac.za
[2] Livermore Software Technology Corporation, 7374 Las Positas Rd, Livermore, CA 94550, USA
nielen@lstc.com
[3]Advanced Vehicle Engineering, DaimlerChrysler Corporation
800 Chrysler Drive East, Auburn Hills, MI 48326, USA
dad41@daimlerchrysler.com
[4]Quantum Consultants, Inc., East Lansing, USA

*Professor. Currently on sabbatical leave at Livermore Software Technology Corporation.

Abstract

This paper describes the multidisciplinary design optimization of a full vehicle to minimize mass while complying with crashworthiness and Noise, Vibration and Harshness (NVH) constraints. A full frontal impact is used for the crashworthiness simulation in the nonlinear dynamics code, LS-DYNA. The NVH constraints are evaluated from an implicit modal analysis of a body-in-white vehicle model using LS-DYNA. Seven design variables describe the structural components of which the thickness can be varied. The crashworthiness constraints relate to crush energy and displacement, while the torsional frequency characteristics are obtained from the modal analysis. The Multidisciplinary Feasible (Fully Integrated) formulation, in which full sharing of the variable sets is employed, is used as the reference case. In an attempt to investigate global optimality, three starting designs are used. Based on a Design of Experiments analysis of variance of the fully-shared variable results for each starting design, discipline-specific variables are selected from the full set using the sensitivity of the disciplinary responses. The optimizer used in all cases is the Successive Response Surface Method as implemented in LS-OPT. It is shown that partial sharing of the variables not only reduces the computational cost in finding an optimum due to fewer, more sensitive variables, but also leads to a better result. The mass of the vehicle is reduced by 4.7% when starting from an existing baseline design, and by 2.5% and 1.1% when starting from a lightest and heaviest starting design respectively.

Introduction

Although still in its infancy, mathematical optimization techniques are increasingly being applied to the crashworthiness design of vehicles. Early crashworthiness studies of the mid 1980's were followed by response surface-based design optimization studies in the 1990's for occupant safety[1,2], component-level optimization[3-5], airbag-related parameter identification[6] and for a full-vehicle simulation[7-9]. These studies focus on one single discipline in the simulation, that of the nonlinear dynamics of the crash event. There is increasing interest in the coupling of other disciplines into the optimization process, especially for complex engineering systems like aircraft and automobiles[10]. The aerospace industry was the first to embrace multidisciplinary design optimization (MDO)[11-13], because of the complex integration of aerodynamics, structures, control and propulsion during the development of air- and spacecraft. The automobile industry has followed suit[14-16]. In Ref.14, the roof crush performance of a vehicle is coupled to its Noise, Vibration and Harshness (NVH) characteristics (modal frequency, static bending and torsion displacements) in a mass minimization study, while Ref.15 extends the study in Ref.14 to include other crash modes, i.e., full frontal and 50% frontal offset impact. Ref. 16 considers the impact of a bumper beam coupled with a bound on its first natural frequency.

Different methods have been proposed when dealing with MDO. The conventional or standard approach is to evaluate all disciplines simultaneously in one integrated objective and constraint set by applying an optimizer to the multidisciplinary analysis (MDA), similar to that followed in single-discipline optimization. The standard method has been called multidisciplinary feasible (MDF), as it maintains feasibility with respect to the MDA. A number of MDO formulations are aimed at decomposing the MDF problem. Concentrating here on hierarchical or structural decomposition (for non-hierarchical including partitioning approaches refer to e.g. Ref.10 and Ref.19), the formulation usually consists of multiple levels.

The objective function, i.e. the criterion that is minimized in crashworthiness optimization, and constraints on the optimization, have mostly been related to occupant safety. E.g. the Head Injury Criterion[2] is used as objective in Refs.1 and 15, while maximum knee force or a femur force-related criterion is used to drive the design optimization in Ref.5. Criteria related to other body parts are the Rib Deflection Criterion or Viscous Criterion (rib cage), the Abdomen Protection Criterion (abdominal area) and Pelvis Performance Criterion (pelvic area)[3]. Other objectives or constraints are related to structural integrity during a crash. Examples are intrusion kinematics (displacement, velocity or acceleration), and the crush history, e.g. in a multi-stage form of the acceleration versus displacement history. The selection depends on the design criteria and type of crash, e.g., side impact, full and partially offset frontal impact or roof crush. In an MDO sense, one would use an overall design objective as the objective function. An obvious choice is the total vehicle mass or the mass of the parts being designed, as it impacts positively on material cost, manufacturing cost and operating cost. The other candidates listed above would then enter the optimization problem as constraints to ensure a safe, lightweight vehicle.

As far as design variables are concerned, these have mainly been geometrical in nature in crashworthiness studies. E.g., in Ref.2, airbag and seat belt variables are used, while in Ref.5, gages and radii of brackets and the yoke of a knee-bolster system are optimized. In Ref.12, the thickness and stiffness of a variety of vehicle subcomponents make up the 19 NVH-only, 10 crash-only and 10 discipline-shared design variables. In the current study, all of the variables relate to thickness or gage.

As this is the first MDO study using LS-OPT, it has as its aim the provision of a benchmark for further studies. For this reason the MDF formulation is chosen in this paper. The MDF formulation layout as customized for the current disciplines is shown in Figure 1. As the current study uses response surfaces in the optimization process, the different disciplines could have different experimental designs and partially shared design variables in general.

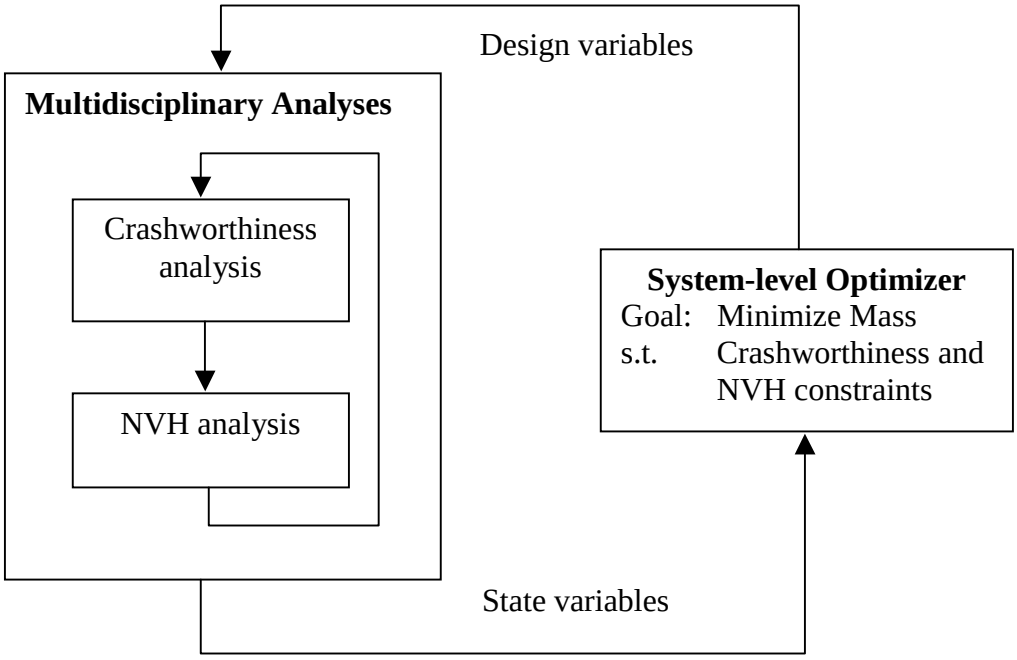

Figure 1 – Multidisciplinary feasible (MDF) MDO architecture

Methodology

MDO modifications to LS-OPT[31]

When applying SRSM to MDF, discipline-specific experimental designs and variable sets are allowed. After each iteration, the variables that are not shared are updated to ensure a unique intermediate design and multidisciplinary feasibility.

Variable screening

As the MDO problem solution cost and coupling depends directly on the way in which variables are shared, a design of experiments (DOE) Analysis of Variance (ANOVA) study is first performed using LS-OPT[24] to determine the significant variables for each discipline. The variance of each variable with respect to each response fitted, is tracked and tested for significance using the partial F-test[25] for each response. The importance of a variable is penalized by both a small absolute coefficient value (weight) computed from the regression, as well as by a large uncertainty in the value of the coefficient pertaining to the variable. A 90% confidence level is used to quantify the uncertainty and the variables are ranked based on this level. Since the relative importance of variables can vary as the optimization progresses through the design space, care should be taken not to screen variables prematurely. Non-linearity can affect ranking due to rapid changes of gradients as well as significant modeling error.

Mode tracking

In the NVH analyses below, it is required to control the frequencies of specific modes during the optimization. Because mode switching can occur, i.e. the sequence of a specific mode can trade

places with another mode when sorted by frequency, obtaining the frequency of a specific mode cannot be performed through mode number alone. To track a specific mode, the following modification was made to LS-DYNA[34], the finite element solver used in this study.

The frequencies of the modes are obtained from a linear modal analysis. The eigenvalues, λ, are obtained from the solution of the linear system.[35]

$$K\phi=\lambda M\phi \qquad (1)$$

where K is the stiffness and M the mass matrix. The associated eigenvectors, ϕ, describe the mode shape at each frequency, λ. During the optimization, the mode number associated with, say, the torsional frequency, may switch with another mode when the modes are sorted by frequency. This switch may be due to modifications to the design prescribed by the optimizer. When the frequency of a particular mode is included in the optimization problem formulation as either an objective or a constraint, it is therefore desirable to be able to track any mode switching automatically.

In the current study, this is done by performing a scalar product of the mass-orthogonalized eigenvector ($\phi_i^T M\phi_j=\delta_{ij}$, δ_{ij} being the Kronecker delta) associated with the mode of interest in the baseline design, with each of the mass-orthogonalized eigenvectors of the modified design, and finding the maximum scalar product[36]. In this scalar product search, the eigenvectors are weighted by the diagonal of the mass matrix in the following fashion:

$$\max_j \left\{ \left(M_0^{\frac{1}{2}} \phi_0 \right)^T \left(M_j^{\frac{1}{2}} \phi_j \right) \right\} \qquad (2)$$

with M_0 and M_j denoting matrices containing the diagonal elements of the mass matrices for the baseline mode and mode j respectively. The maximum scalar product would indicate the mode most similar in shape to the baseline mode (parallel vectors having a scalar product of unity). Having identified this mode, the associated eigenvalue or frequency, as well as the new mode number, can be returned to the optimizer.

Optimization

The successive response surface method is applied as described in e.g. References 32 and 33.

Full frontal crash and NVH optimization

Modeling

The crashworthiness simulation considers a model containing approximately 30 000 elements of a National Highway Transportation and Safety Association (NHTSA) vehicle[37] undergoing a full frontal impact. A modal analysis is performed on a so-called 'body-in-white' model containing approximately 18 000 elements. The crash model for the full vehicle is shown in Figure 2 for the undeformed and deformed (time = 78ms) states, and with only the structural components affected by the design variables, both in the undeformed and deformed (time = 72ms) states, in Figure 3. The NVH model is depicted in Figure 4 in the first torsion vibrational mode. Only body parts that are crucial to the vibrational mode shapes are retained in this model. The design variables are all thicknesses or gages of structural components in the engine compartment of the vehicle (Figure 3), parameterized directly in the LS-DYNA[34] input file. Twelve parts are affected, comprising aprons, rails, shotguns, cradle rails and the cradle cross member (Figure 3). LS-DYNA v.960[34] is used for both the crash and NVH simulations, in explicit and implicit modes respectively.

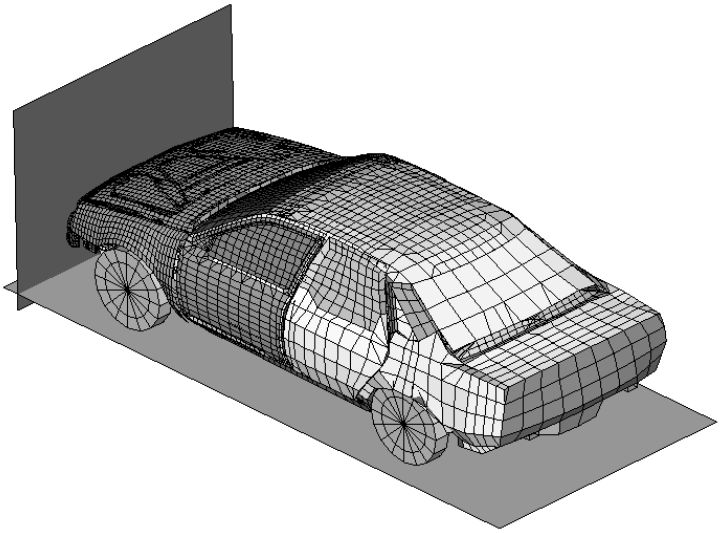

(a)

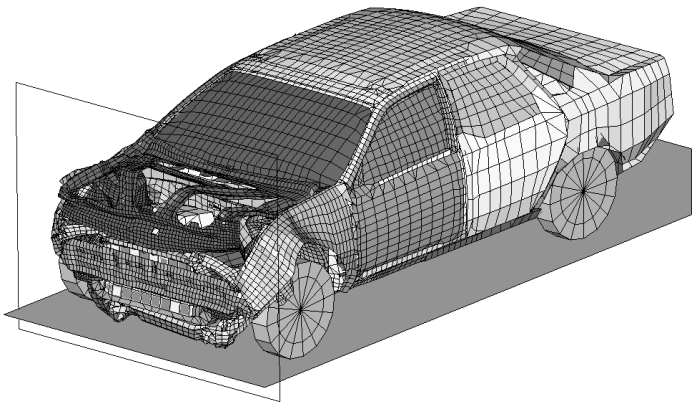

(b)

Figure 2 – Crash model of vehicle showing road and wall
(a) Undeformed (b) Deformed (78ms)

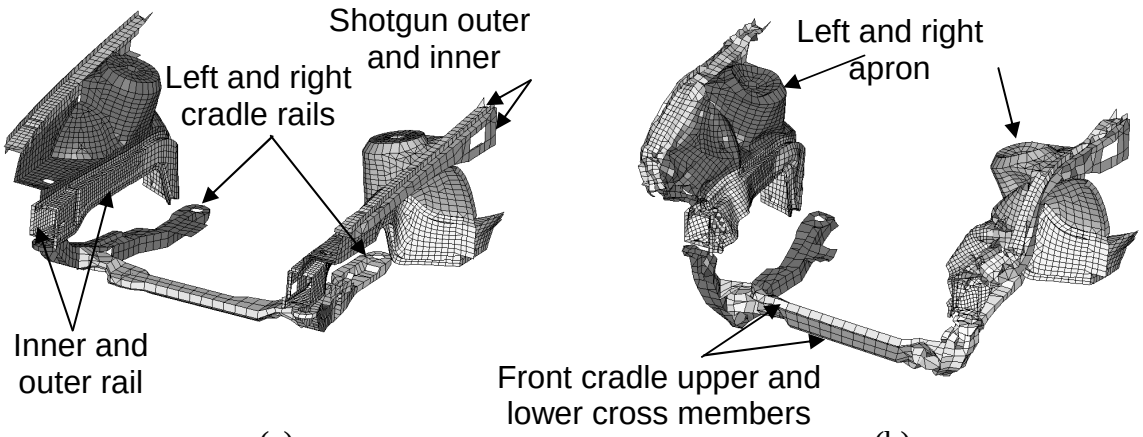

Figure 3 – Structural components affected by design variables – (a) Undeformed and (b) deformed (time = 72ms)

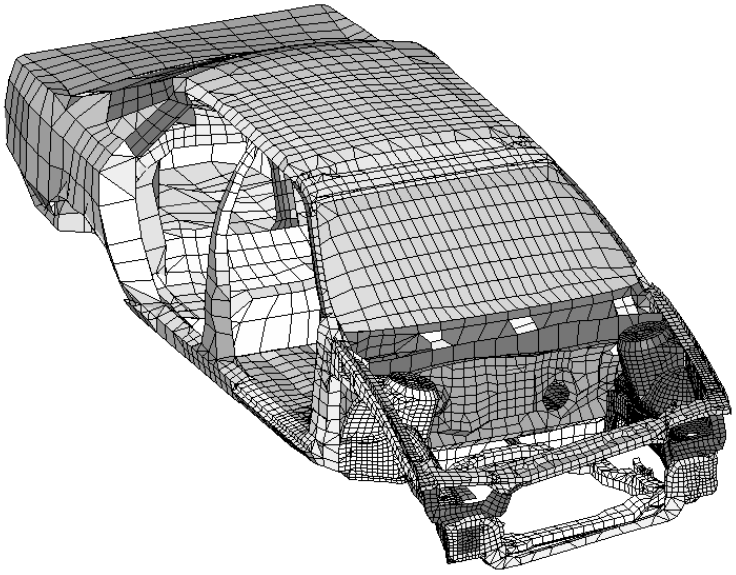

Figure 4 – Body-in-white model of vehicle in torsional vibration mode (38.7Hz)

Formulation of optimization problem (MDF formulation)

The optimization problems for the different starting designs considered are defined as follows:

Fully-shared variables – Starting design 1 (Baseline):

Minimize Mass (3)

s.t. Maximum displacement($\boldsymbol{x}_{crash}$) > 551.8mm
Stage 1 pulse($\boldsymbol{x}_{crash}$) > 14.34g
Stage 2 pulse($\boldsymbol{x}_{crash}$) > 17.57g
Stage 3 pulse($\boldsymbol{x}_{crash}$) > 20.76g
37.77Hz < Torsional mode frequency($\boldsymbol{x}_{NVH}$) < 39.77Hz

with $\boldsymbol{x}_{crash} = \boldsymbol{x}_{NVH}$ = [*rail_inner, rail_outer, cradle_rails, aprons, shotgun_inner, shotgun_outer, cradle_crossmember*]^T.

Partially-shared variables – Starting design 1 (Baseline):
Minimize Mass (4)
s.t. Maximum displacement($\boldsymbol{x}_{crash}$) = 551.8mm
Stage 1 pulse($\boldsymbol{x}_{crash}$) > 14.34g
Stage 2 pulse($\boldsymbol{x}_{crash}$) > 17.57g
Stage 3 pulse($\boldsymbol{x}_{crash}$) > 20.76g
38.27Hz < Torsional mode frequency($\boldsymbol{x}_{NVH}$) < 39.27Hz
with $\boldsymbol{x}_{crash}$ [*rail_inner, rail_outer, cradle_rails, aprons, shotgun_inner, shotgun_outer*]^T;
$\boldsymbol{x}_{NVH}$ = [*cradle_rails, shotgun_inner, shotgun_outer, cradle_crossmember*]^T.

Partially-shared variables – Starting design 2 (Minimum weight):
Minimize Mass (5)
s.t. Maximum displacement($\boldsymbol{x}_{crash}$) = 551.8mm
Stage 1 pulse($\boldsymbol{x}_{crash}$) > 14.34g
Stage 2 pulse($\boldsymbol{x}_{crash}$) > 17.57g
Stage 3 pulse($\boldsymbol{x}_{crash}$) > 20.76g
38.27Hz < Torsional mode frequency($\boldsymbol{x}_{NVH}$) < 39.27Hz
with $\boldsymbol{x}_{crash}$ [*rail_inner, rail_outer, cradle_rails, aprons*]^T;
$\boldsymbol{x}_{NVH}$ = [*cradle_rails, shotgun_inner, shotgun_outer, cradle_crossmember*]^T.

Partially-shared variables – Starting design 3 (Maximum weight):
Minimize Mass (6)
s.t. Maximum displacement($\boldsymbol{x}_{crash}$) = 551.8mm
Stage 1 pulse($\boldsymbol{x}_{crash}$) > 14.34g
Stage 2 pulse($\boldsymbol{x}_{crash}$) > 17.57g
Stage 3 pulse($\boldsymbol{x}_{crash}$) > 20.76g
38.27Hz < Torsional mode frequency($\boldsymbol{x}_{NVH}$) < 39.27Hz
with $\boldsymbol{x}_{crash}$ [*rail_inner, rail_outer, cradle_rails, aprons, shotgun_inner, shotgun_outer, cradle crossmember*]^T;
$\boldsymbol{x}_{NVH}$ = [*cradle_rails, shotgun_inner, shotgun_outer, cradle_crossmember*]^T.

The different variable sets in Equations (4-6) were obtained from ANOVA studies. See Reference 33 for more detail. The Mass objective in each case incorporates all the components defined in Figure 3. The allowable torsional mode frequency band is reduced to 1Hz for the partially-shared cases to provide an optimum design that is more similar to the baseline. The maximum displacement constraint is changed from an inequality constraint (Equation (3)) to an equality constraint in Equations (4-6) in an attempt to force the optimizer to better maintain the intrusion of the baseline design. This is especially required for the minimum weight starting design, where the intrusion is expected to initially be much higher than the baseline value.

The three stage pulses are calculated from the SAE filtered (60Hz) acceleration[34] and displacement of a left rear sill node in the following fashion:

$$\text{Stage } i \text{ pulse} = -k\int_{d_1}^{d_2} a\,dx \text{ ; } k = 0.5 \text{ for } i = 1, 1.0 \text{ otherwise;} \quad (7)$$

with the limits (d_1;d_2) = (0;184); (184;334); (334;Max(displacement)) for i = 1,2,3 respectively, all displacement units in mm and the minus sign to convert acceleration to deceleration. The Stage 1 pulse is represented by a triangle with the peak value being the value used.

In summary, the optimization problem has as its aim the minimization of the mass while maintaining the baseline characteristics of the model, i.e. not degrading its crush energy, intrusion or torsional frequency characteristics. A left rear sill node is used to monitor the displacement. The constraints are scaled using the target values to balance the violations of the different constraints. This scaling is only important in cases where multiple constraints are violated as in the current problem.

Results and discussion

Simulation results

The deceleration versus displacement curves of the baseline crash model and Iteration 9 design are shown in Figure 6 for the partially-shared variable case. The stage pulses as calculated by Equation 4 are also shown, with the optimum values only differing slightly from the baseline. The reduction in displacement at the end of the curve shows that there is spring-back or rebound at the end of the simulation.

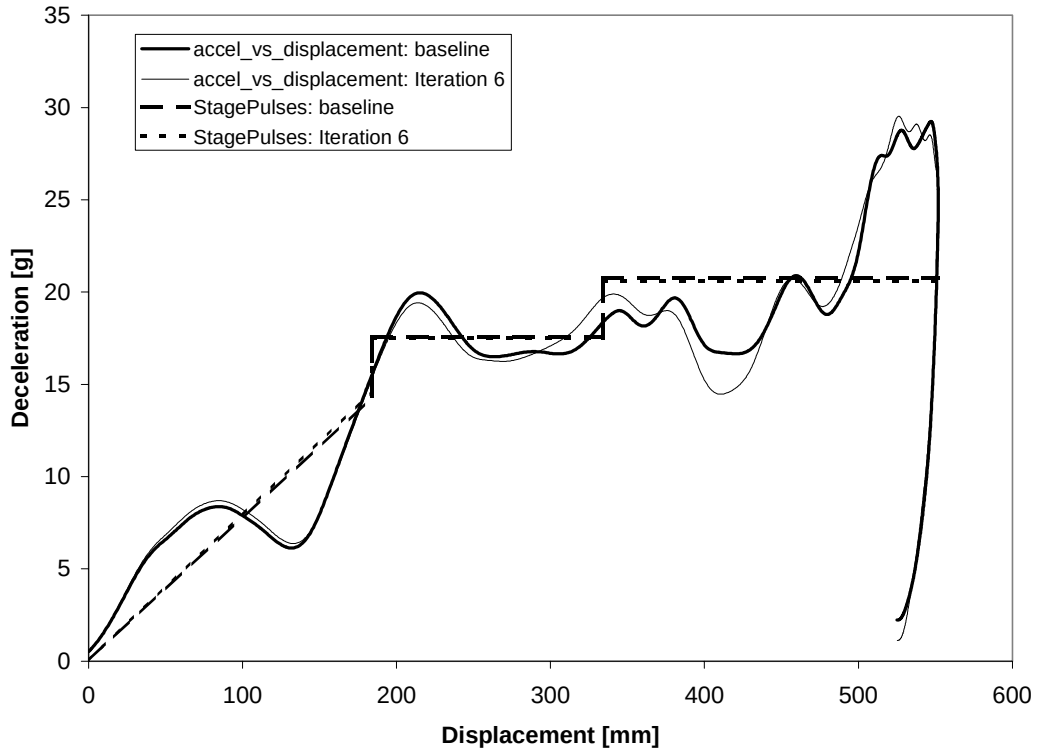

Figure 5 – Deceleration (Filtered: SAE 60Hz) versus displacement of baseline and Iteration 6 design – (Partially-shared variables): Starting design 1

Optimization history results

The bounds on the design variables are given in Table 1 together with the different initial designs or starting locations used. Starting design 1 corresponds to the baseline model as shown in Figures 2 through 4, while the other two designs correspond to the opposite corners of the design

space hypercube, i.e. the lightest design and heaviest design possible with the design variables used.

Beginning with starting design 1, the optimization history of the objective and constraints are shown for both cases in Figures 6 through 9 for starting design 1. Most of the reduction in mass occurs in the first iteration (Figure 6), although this results in a significant violation of the maximum displacement and second stage pulse constraints, especially in the fully-shared variable case. The second iteration corrects this, and from here the optimizer tries to reconcile four constraints that are marginally active. Most of the intermediate constraint violations (see e.g. Figure 7) can be ascribed to the difference between the value predicted by the response surface and the value computed by the simulation. The torsional frequency remains within the bounds set during the optimization for the full-shared case.

	Rail_inner [mm]	Rail_outer [mm]	Cradle rail [mm]	Aprons [mm]	Shotgun inner [mm]	Shotgun outer [mm]	Cradle cross member [mm]
Lower bound	1	1	1	1	1	1	1
Upper bound	3	3	2.5	2.5	3	3	2.5
Starting design 1 (Baseline)	2	1.5	1.93	1.3	1.3	1.3	1.930
Starting design 2 (Minimum weight)	1	1	1	1	1	1	1
Starting design 3 (Maximum weight)	3	3	2.5	2.5	3	3	2.5

Table 1 – Bounds on design variables and starting designs for optimization

The results of the partially-shared variable case for starting design 1 (Figure 6) can be seen to be superior to the fully-shared case. The reason for this is that all the disciplinary responses are now sensitive to their respective variables, allowing faster convergence. Interestingly, most of the mass reduction in this case occurs in the cradle cross member, a variable that is only included in the NVH simulation. The variation of the remaining variables is however enough to meet all the crash constraints. The reduction in the allowable frequency band made the NVH performance more interesting in Phase 1 than Phase 2. It can be seen in Figure 11 that the lower bound becomes active during the optimization process, but that the optimizer then pulls the torsional mode frequency within the prescribed range. The final design iteration considered (iteration 9) was repeated (see point 10 in Figures 6 through 9) with the variables rounded to the nearest 0.1mm due to the 0.1mm manufacturing tolerance typically used in the stamping of automotive parts. It is shown that the design is lighter by 4.75% from the baseline, but at the cost of a 2.4% violation in the Stage 2 pulse. The other constraints are satisfied.

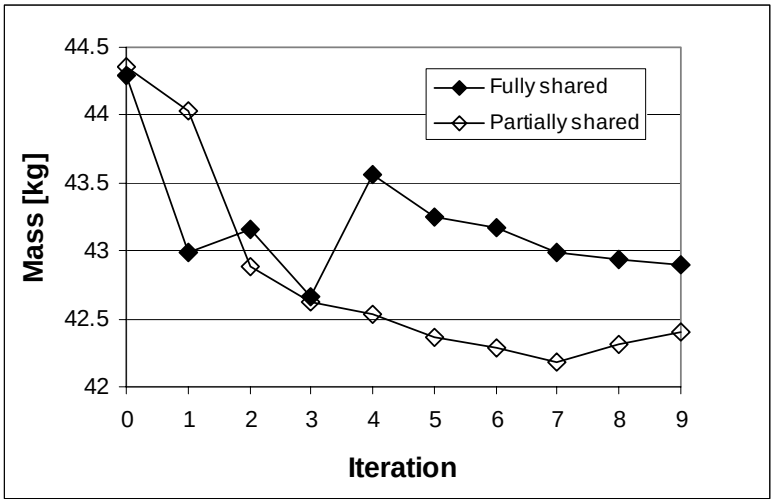

Figure 6 – Optimization history of component mass (Objective) – Starting design 1

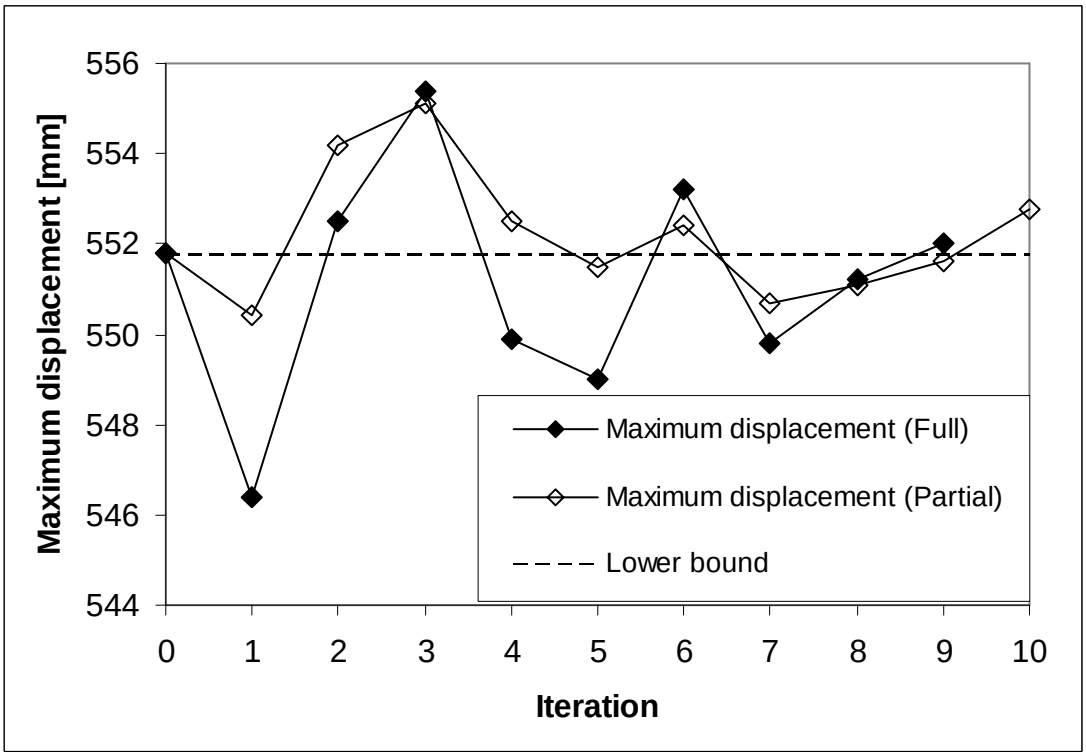

Figure 7 – Optimization history of maximum displacement – Starting design 1

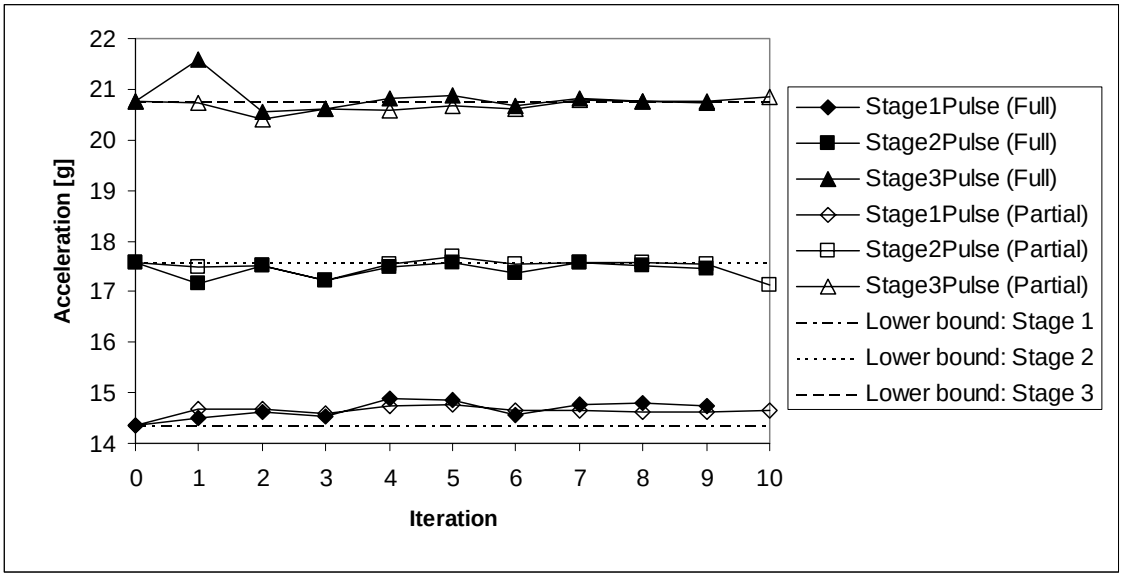

Figure 8 – Optimization history of Stage pulses – Starting design 1

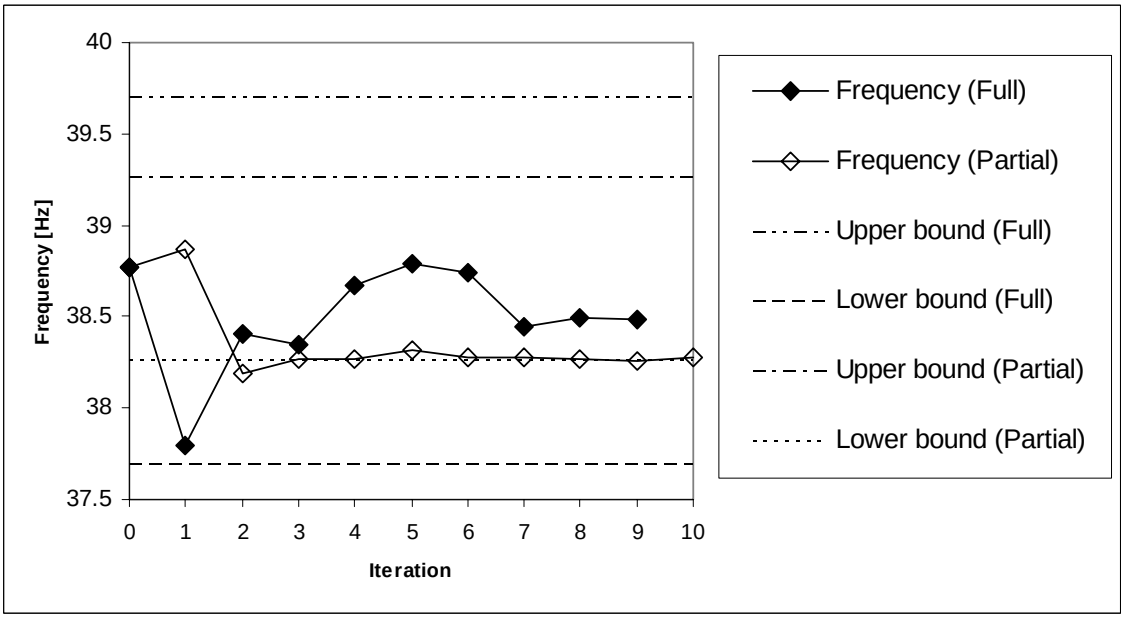

Figure 9 – Optimization history of torsional mode frequency – Starting design 1

The results for the heaviest and lightest starting designs (2 and 3) are given in Figures 10 through 13. In both cases, an ANOVA was performed after one iteration of full sharing only in order to reduce the discipline-specific variables. The optimization was then restarted using the variable sets as defined in Equations (5) and (6). As expected, both designs converge to an intermediate mass in an attempt to satisfy all the constraints. The heaviest design history exhibits the largest mass change because of the significant increase in the thickness of the components over the baseline design.

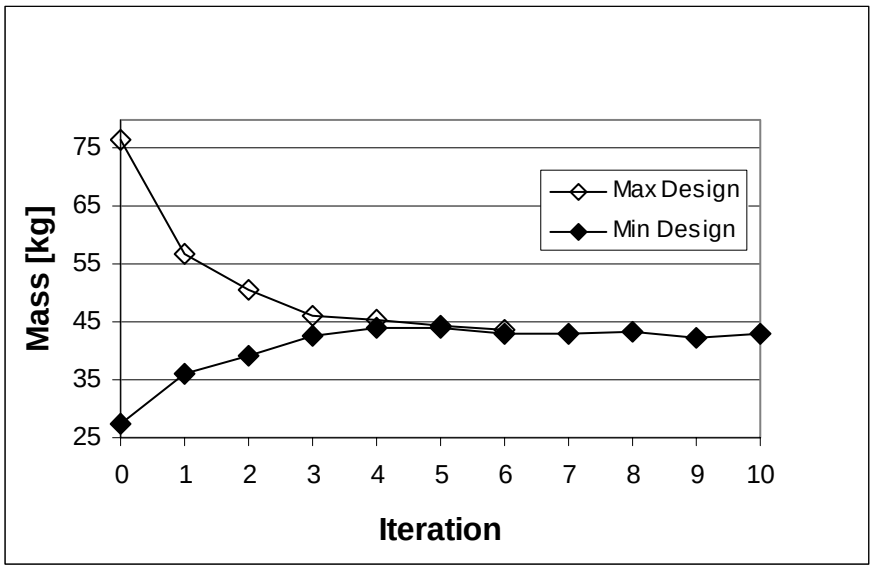

Figure 10 – Optimization history of component mass (Objective) – Starting designs 2 and 3

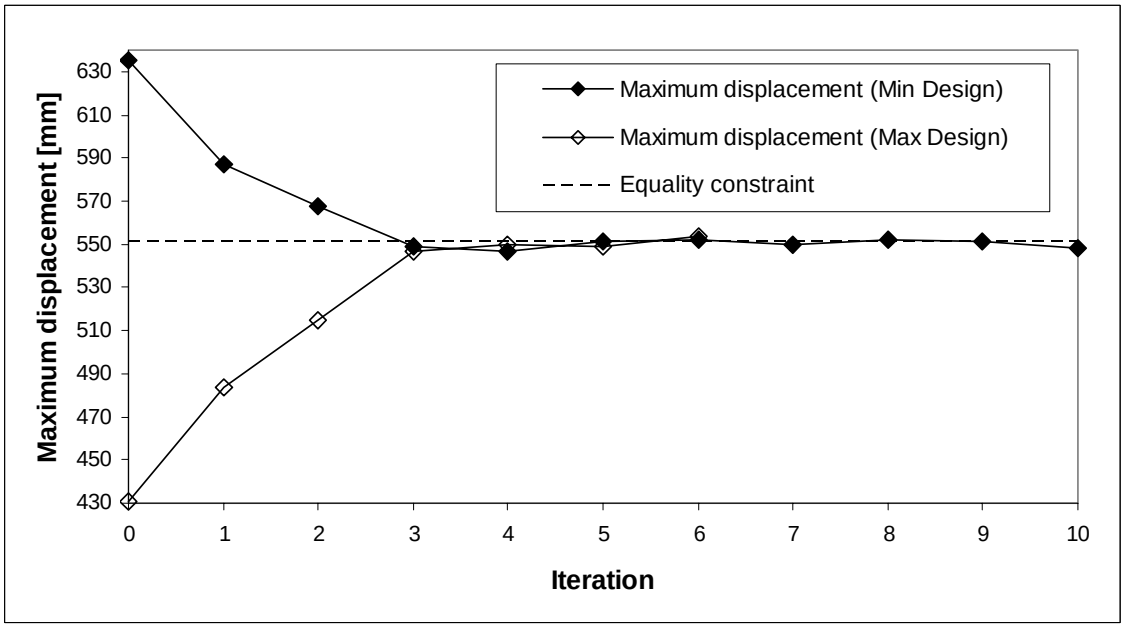

Figure 11 – Optimization history of maximum displacement – Starting designs 2 and 3

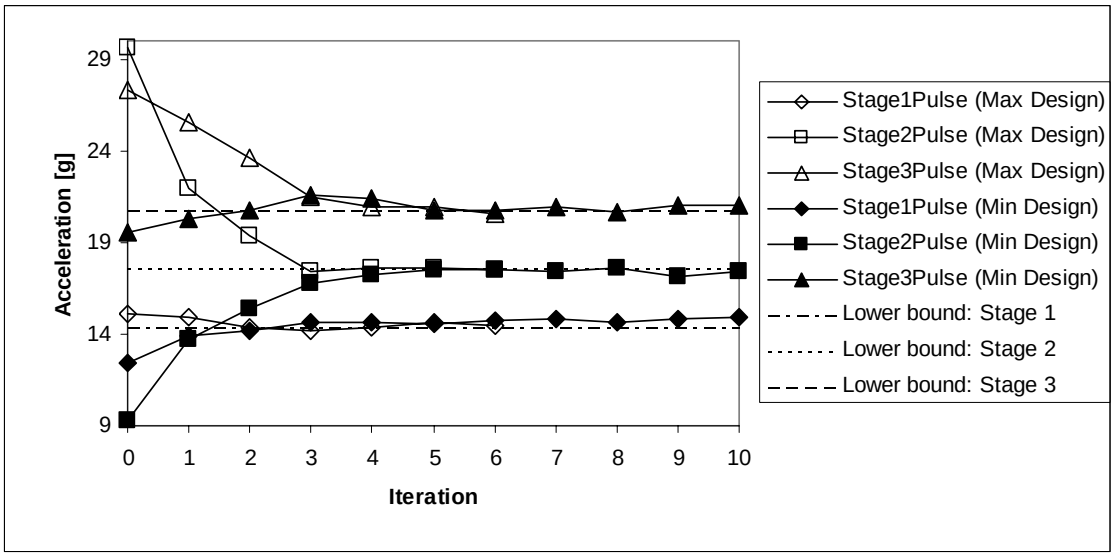

Figure 12 – Optimization history of Stage pulses – Starting designs 2 and 3

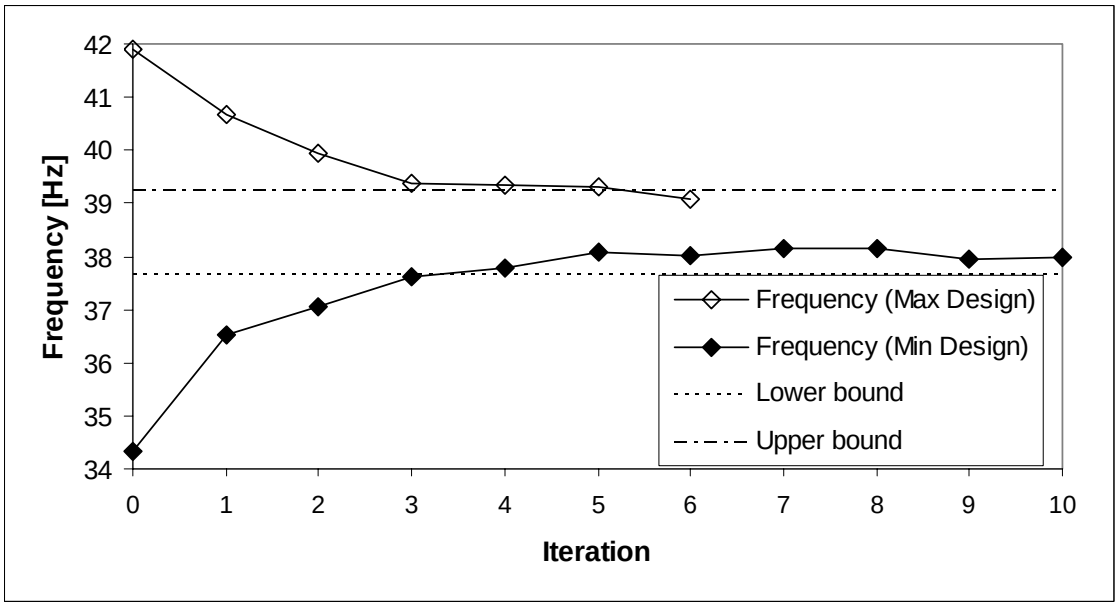

Figure 13 – Optimization history of torsional mode frequency – Starting designs 2 and 3

Comparison of optimum designs

The optimum designs obtained in each case above are compared in Table 6 for the objective function and constraints, and in Table 7 for the design variables. Note how the partially shared variable Starting design 1 case has the lowest mass while performing the best as far as the constraints are concerned. After rapidly improving from the initial violations, both the extreme starting designs converged to local minima. The maximum design (Starting design 3) started the furthest away from the optimum design, but converged rapidly due to the increased initial move limit. All the designs converge to different design vectors, with different combinations of the component thicknesses resulting in similar performance.

	Case	It. No.	Mass [kg]	Maximum displacement [mm]	Stage 1 pulse [g]	Stage 2 pulse [g]	Stage 3 pulse [g]	Frequency [Hz]
Constraint				551.8	14.34	17.57	20.76	[37.77;39.77] or [38.27;39.27]
Fully shared	Starting design 1 (base)	9	42.9	552.0	14.74	17.46	20.73	38.48
Partially shared	Starting design 1 (base)	9	42.4	551.6	14.62	17.53	20.77	38.26
	Starting design 2 (min)	8	43.2	552.5	14.66	17.56	20.69	38.15
	Starting design 3 (max)	6	43.8	553.7	14.46	17.48	20.61	39.07

Table 6 – Comparison of objective and constraints for all optimization cases

	Case	Rail_inner [mm]	Rail_outer [mm]	Cradle rail [mm]	Aprons [mm]	Shotgun inner [mm]	Shotgun outer [mm]	Cradle cross member [mm]
Fully shared	Starting design 1 (base)	2.322	1.286	1.842	1.158	1.196	1.614	1.486
Partially shared	Starting design 1 (base)	1.948	1.475	1.275	1.992	1.346	1.383	1
	Starting design 2 (lightest)	2.04	1.884	1.507	1.441	1.11	1.372	1.161
	Starting design 3 (heaviest)	1.95	1.765	1.469	1.303	2.123	1.391	1.208

Table 7 – Comparison of optimum design variables for all optimization cases

Convergence and computational cost

Comparing the fully- and partially-shared variable cases for starting design 1, it can be seen that the optimization process converged in 9 iterations in the first case, while in the latter, a good compromised design was found in only 6 iterations. Coupled to the reduction in design variables, especially for the NVH simulations, the reduction in the number of simulations as shown in Table 8 is the result. To explain the number of simulations, clarification of the experimental design used is in order. A 50% over-sampled *D*-optimal experimental design is used, whereby the number of experimental points for a linear approximation is determined from the formula: $1.5(n + 1) + 1$, where n refers to the number of design variables. Consequently, for the full sharing, 7 variables imply 13 experimental design points, while for the partial sharing, 6 variables for crash imply 11 design points, and 4 variables for NVH imply 8 points[24]. The NVH simulations, although not time-consuming due to their implicit formulation, involve a large use of memory due to double-precision matrix operations. Crashworthiness simulations, on the other hand, require little memory because of single-precision vector operations, but are time-consuming due to their explicit nature. It is therefore preferable to assign as many processors as

possible to the crashworthiness simulations, while limiting the number of simultaneous NVH simulations to the available computer memory to prevent swapping.

Case	Number of crash simulations for 'convergence'	Number of NVH simulations for 'convergence'
Fully-shared variables	9 x 13 = 127	9 x 13 = 127
Partially-shared variables	6 x 11 = 66	6 x 8 = 48

Table 8 – Number of simulations for Fully- and Partially-Shared Variable Cases (Starting design 1)

Conclusions

The paper describes the multidisciplinary feasible optimization of a full vehicle model considering crashworthiness and NVH design criteria. LS-OPT is used for the optimization. Using partially shared variables, a component mass reduction of almost 5% is achieved while maintaining or improving the design criteria of the baseline design.

The optimization using partially shared variables converges more rapidly than when using fully shared variables, probably because of the elimination of uncertain variables using the ANOVA method based on the partial F-test. It is shown that the optimizer finds different optima when starting from different designs located in the extreme (minimum and maximum weight) corners of the design space.

It is possible that a mode that is identified in the baseline design can become sufficiently obscured by the modes of a modified design. This happened in the case (maximum weight starting design) where the starting design was far away from the anticipated optimum design. A remedy could be to monitor intermediate designs to update the baseline vibration mode.

Acknowledgements

The authors would like to thank DaimlerChrysler for the use of their computing facilities for part of this study. They would like to acknowledge the support from the South African National Research Foundation, Grant no. GUN2046904, for the sabbatical of the first author at the Livermore Software Technology Corporation from the University of Pretoria, South Africa. The authors are also indebted to Suri Balasubramanyam of LSTC for assisting with the collaboration between LSTC and DaimlerChrysler. The computational resources used in this study included Compaq Alpha, IBM SP, and Hewlett Packard V-Class computers.

References

1. Etman LFP. Optimization of Multibody Systems using Approximation Concepts. Ph.D. thesis, Technical University Eindhoven, The Netherlands 1997.
2. Etman LFP, Adriaens JMTA, van Slagmaat MTP, Schoofs AJG, Crashworthiness Design Optimization using Multipoint Sequential Linear Programming. *Structural Optimization* 1996; **12**:222-228.
3. Marklund P-O. Optimization of a Car Body Component Subjected to Impact. Linköping Studies in Science and Technology, Thesis No. 776, Department of Mechanical Engineering, Linköping University, Sweden 1999.
4. Marklund P-O., Nilsson L. Optimization of a Car Body Component Subjected to side Impact. *Struct Multidisc Optim*. 2001 **21**:383-392.
5. Akkerman A, Thyagarajan R, Stander N, Burger M, Kuhn R, Rajic H. Shape Optimization for Crashworthiness Design using Response Surfaces. *Proceedings of the International Workshop on Multidisciplinary Design Optimization*. Pretoria, South Africa, August 8-10, 2000, pp. 270-279.
6. Stander N. Optimization of Nonlinear Dynamic Problems using Successive Linear Approximations. AIAA Paper 2000-4798, 2000.
7. Schramm U, Thomas H. Crashworthiness design using structural optimization. *AIAA Paper* 98-4729, 1998.
8. Gu L. A comparison of polynomial based regression models in vehicle safety analysis. *Paper* DETC2001/DAC-21063. *Proceedings of DETC'01 ASME 2001 Design Engineering Technical Engineering Conferences and the Computers and Information in Engineering Conference.* Pittsburgh, PA. September 9-12, 2001.
9. Yang R-J, Wang N, Tho CH, Bobineau JP, Wang BP. Metamodeling development for vehicle frontal impact simulation. *Paper* DETC2001/DAC-21063. *Proceedings of DETC'01 ASME 2001 Design Engineering Technical Engineering Conferences and the Computers and Information in Engineering Conference.* Pittsburgh, PA. September 9-12, 2001.
10. Lewis K, Mistree F. The other side of multidisciplinary design optimization: accommodating a mutiobjective, uncertain and non-deterministic world. *Engineering Optimization* 1998 **31**:161-189.
11. Barthelemy J-F,M. (1983) Development of a multilevel optimization approach to the design of modern engineering systems. NASA/CR-172184-1983.
12. Haftka RT, Sobieszczanski-Sobieski J. Multidisciplinary aerospace design optimization: Survey of recent developments. *AIAA Paper* 96-0711, 1996.
13. Sobieszczanski-Sobieski J, Haftka RT. Multidisciplinary Aerospace Design Optimization: Survey of recent developments, *Structural Optimization* 1997; **14**(1):1-23.
14. Sobieszczanski-Sobieski J, Kodiyalam S, Yang R-J. Optimization of car body under constraints of noise, vibration, and harshness (NVH), and crash. *AIAA Paper* 2000-1521, 2000.
15. Yang R-J, Gu L, Tho CH, Sobieszczanski-Sobieski J. Multidisciplinary design optimization of a full vehicle with high performance computing. *AIAA Paper* 2001-1273, 2001.
16. Schramm U. Multi-disciplinary optimization for NHV and crashworthiness. *Proceedings of the First MIT Conference on Computational Fluid and Solid Mechanics*. Bathe KJ, Ed., Boston, June 12-15, 2001. Elsevier Science Ltd., Oxford, pp.721:724.
17. Alexandrov NM, Lewis RM. Analytical and computational properties of distributed approaches to MDO. AIAA Paper 2000-4718, 2000.

18. Alexandrov NM, Lewis RM. Algorithmic perspectives on problem formulations in MDO. AIAA Paper 2000-4719, 2000.
19. Michelena N, Papalambros PY. A network reliability approach to optimal decomposition of design problems. *ASME Journal of Mechanical Design* 1995; **117**(3):433-440.
20. Haftka RT, Gürdal A, Kamat MP. Elements of structural optimization. Kluwer Academic Publishers, Dordrect, 1990.
21. Cramer EJ, Dennis JE Jr, Frank PD, Lewis RM, Shubin GR. Problem formulations for multidisciplinary optimization. *SIAM Journal of Optimization* 1994; **40**(4):754-776.
22. Zang TA, Green LL. Multidisciplinary Design Optimization techniques: Implications and opportunities for fluid dynamics research. AIAA Paper 99-3798, 1999.
23. Salas AO, Townsend JC. Framework Requirements for MDO Application Development, AIAA Paper 98-4740, 1998.
24. Stander N. *LS-OPT User's Manual Version 1*, Livermore Software Technology Corporation, Livermore, CA, 1999.
25. Myers RH, Montgomery DC. *Response Surface Methodology*. Wiley: New York, 1995.
26. Snyman JA. The LFOPC leap-frog algorithm for constrained optimization. *Computers and Mathematics with Applications* 2000; **40**:1085-1096.
27. Stander N, Craig KJ. On the robustness of the successive response surface method for simulation-based optimization. Submitted to *Engineering Computations*. July 2001.
28. Stander, N. "The Successive Response Surface Method Applied to Sheet-Metal Forming", Proceedings of the First MIT Conference on Computational Fluid and Solid Mechanics, Boston, June 12-14, 2001. Elsevier Science Ltd., Oxford.
29. Roux WJ, Stander N, Haftka RT. Response surface approximations for structural optimization. *International Journal for Numerical Methods in Engineering* 1998; **42**:517-534.
30. Haftka RT, Gürdal Z. *Elements of Structural Optimization*. Kluwer: Dordrecht, 1990, p.257.
31. Stander N, Craig KJ. *LS-OPT User's Manual Version 2*, Livermore Software Technology Corporation, Livermore, CA, 2001.
32. Stander N, Craig KJ. On The Robustness of a Simple Domain Reduction Scheme for Simulation-Based Optimization. *Eng. Comput., Submitted.*
33. Craig KJ, Stander N, Dooge D and Varadappa S. Multidisciplinary Design Optimization of Automotive Crashworthiness and NVH using Response Surface Methods. *AIAA Journal., Submitted.*
34. Livermore Software Technology Corporation. *LS-DYNA manual version 960*. Livermore, CA, 2001.
35. Bathe K-J, Wilson EL. *Numerical Methods in Finite Element Analysis*. Prentice-Hall: Inglewood Cliffs, New Jersey, 1976, chapter 10.
36. Hallquist JO. Private communication, 2001.
37. National Crash Analysis Center (NCAC). Public Finite Element Model Archive, www.ncac.gwu.edu/archives/model/index.html 2001.